# Aggregation Models of Potential Cyclical Trimethylsulfonium Dicyanamide Ionic Liquid Clusters

**W. Robert Carper,*,† Kevin Langenwalter,† Naveed S. Nooruddin,† Michael J. Kullman,† Dirk Gerhard,‡ and Peter Wasserscheid‡**

*Department of Chemistry, Wichita State University, Wichita, Kansas 67260-0051, and Lehrstuhl für Chemische Reaktionstechnik, Universität Erlangen-Nürnberg, Egerlandstrasse 3, Erlangen, D-91058, Germany*

*Received: October 17, 2008; Revised Manuscript Received: December 9, 2008*

Raman and infrared spectra of trimethylsulfonium dicyanamide [$(CH_3)_3SN(CN)_2$] are reported and accurately reproduced by DFT methods (B3LYP and B3PW91), MP2, and MP3, and to a lesser extent by the RHF method. The $(CH_3)_3SN(CN)_2$ ionic liquid forms two isomeric dimers that are of cyclic structure, one of which is 13 kcal/mol lower in energy than the other. Both isomeric cyclic pairs (versions 1 and 2), $[(CH_3)_3SN(CN)_2]_2$, have the potential to further combine and form a common structure containing four pairs of $(CH_3)_3SN(CN)_2$. This structure can then conceivably undergo a stacking procedure to form extended ionic liquid nanotubes of eight ionic liquids, $[(CH_3)_3SN(CN)_2]_8$. The possible formation of gas phase ionic liquid clusters of two, four, and eight trimethylsulfonium dicyanamide ionic liquids is supported by highly exergonic free energy changes obtained from B3LYP/(6-311+G(d,p)) density functional calculations.

## Introduction

Room temperature ionic liquids (RTILs) have generated considerable excitement in recent years as a new type of solvent medium that possesses minimal vapor pressure.[1−4] Ionic liquids can be recycled, thus making synthetic processes less expensive and potentially more efficient and environmentally friendly. The use of ionic liquids has proved beneficial in numerous areas including those of homogeneous and heterogeneous catalyses,[1,2,4] chirality transfer,[5,6] and tribology.[7] As a result of these and other applications,[4] the interest in ionic liquids as a reaction medium has intensified in recent years and has resulted in the reporting of many new ionic liquids including those that contain both organic cations and organic anions such as the trialkysulfonium dicyanamides.[8]

The ability of ionic liquids to form supramolecular aggregates has always been suspected by various investigators, and recent reports in the literature establish this as factual in both liquid and gas phases using mass spectrophotometric, $^1$H NMR, conductivity, microcalorimetric, and photoelectron spectroscopic methods.[9−12] The ability of room temperature ionic liquids to aggregate undoubtedly affects their ability to serve as efficient reaction media and suggests that those methods identifying the aggregation process may prove to be quite useful.>

In recent years, investigators have used ab initio calculations and Raman spectra to probe both the overall and local structure of ionic liquids as outlined in detail in several excellent reviews.[13,14] The advantage of Raman over IR spectra is often due to the complexity of overlapping bands in IR spectra that are difficult to deconvolute. Fortunately, both the Raman and IR spectra of $(CH_3)_3SN(CN)_2$ are relatively simple when compared with other ionic liquids such as the imidzolium−$PF_6^-$ and imidzolium−$BF_4^-$ ionic liquids.[15,16]

In this study, the possible formation of cyclical and ultimately tubular structures of the ionic liquid trimethylsulfonium dicyanamide, $(CH_3)_3SN(CN)_2$, is modeled in the gas phase using theoretical methods that accurately reproduce vibrational spectra. The ability of trimethylsulfonium dicyanamide, $(CH_3)_3SN(CN)_2$, to conceivably form cyclical pairs that in turn aggregate into helical structures is supported by the results of theoretical and spectroscopic studies reported herein. These gas phase models correlate well with static vibrational spectra (Raman and IR) of trimethylsulfonium dicyanamide in a manner similar to results obtained for imidazolium hexafluorophosphate and imidazolium terafluoroborate ionic liquids.[15,16] The trimethylsulfonium dicyanamide theoretical and experimental vibrational spectra correlation is very good and remains at a high level as one models potential aggregates of trimethylsulfonium dicyanamide ionic liquid ion pairs.

## Methods

**Preparation and Measurements.** Trimethylsulfonium dicyanamide was prepared in a stepwise manner.[8] The trimethylsufonium iodide precursor was synthesized using the synthetic approach of Paulsson et al.[17] Equimolar amounts of dimethyl sulfide and methyl iodide dissolved in dry acetone were stirred in darkness at ambient conditions for several days. Silver dicyanamide was precipitated by mixing aqueous solutions of silver nitrate and sodium dicyanamide (1:1 molar ratio). The white residue was filtered off, washed with water to remove any unreacted reagents, and used immediately. An aqueous solution of the iodide was added to

* Corresponding author. E-mail: Bob.Carper@wichita.edu.
† Wichita State University.
‡ Universität Erlangen-Nürnberg.

10.1021/jp809215z CCC: $40.75 
Published on Web 01/22/2009

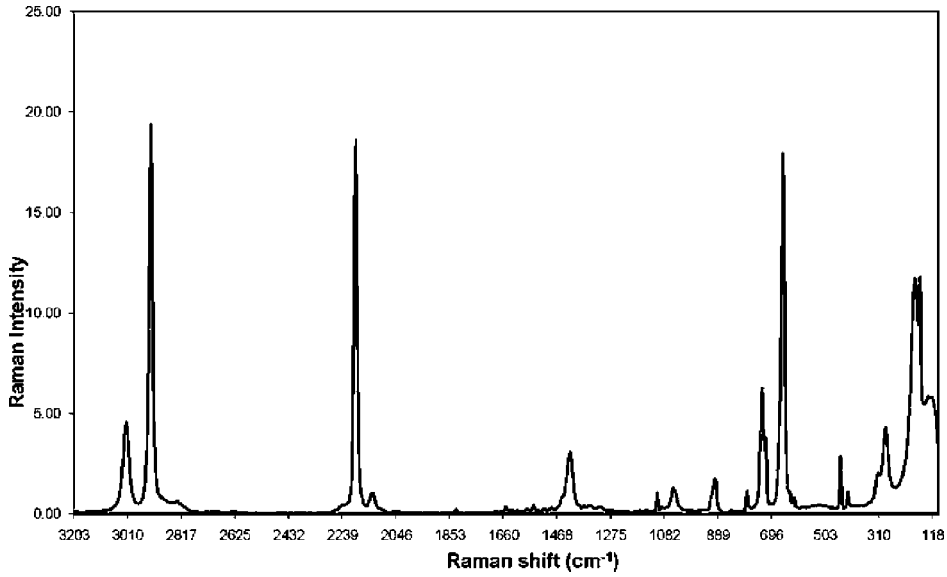


**Figure 1.** Raman spectrum of $(CH_3)_3SN(CN)_2$ at 2 $cm^{-1}$ resolution.

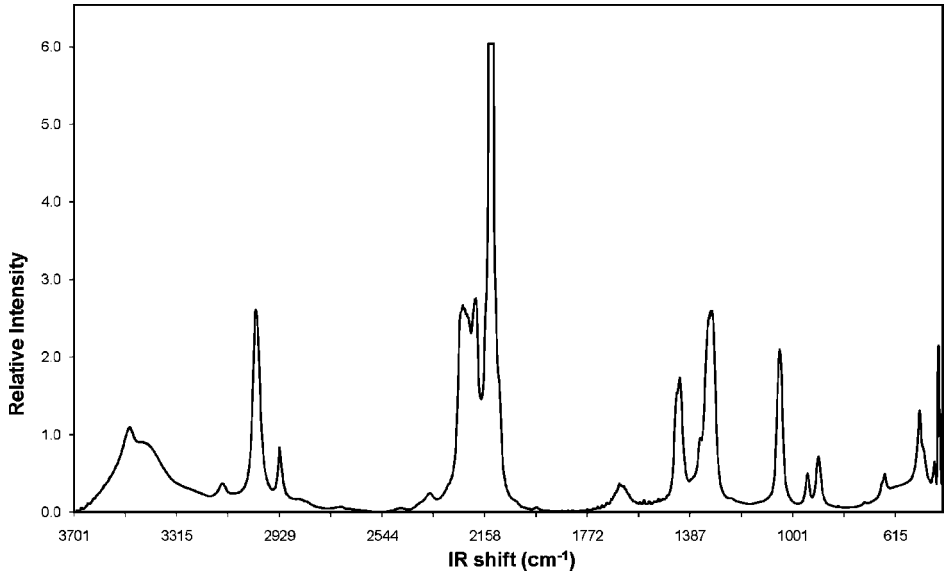


**Figure 2.** IR spectrum of $(CH_3)_3SN(CN)_2$.

an aqueous slurry of the excess (1:1.1) silver dicyanamide, and the solution was heated to 40 °C with stirring overnight. Silver iodide was removed by filtration before drying the product under reduced pressure of 1 mbar. To ensure complete removal of silver salts from the product, the dried ionic liquid was cooled in a freezer overnight before further filtration. Trimethylsulfonium dicyanamide was dried by addition of dry dichloromethane and stirring at 1 mbar and 40 °C overnight.

The Raman spectrum of trimethylsulfonium dicyanamide (Figure 1) was taken using a Nicolet Model 950 Raman spectrophotometer operating at 2 $cm^{-1}$ resolution. The IR spectrum (Figure 2) was obtained with a Nicolet Model 360 FTIR at 2 $cm^{-1}$ resolution.

**Computational Methods.** The ab initio (RHF) and density functional (DFT) calculations were obtained using Gaussian 03 in a tight fit configuration.[18] The calculated vibrational frequencies of all structures contain no imaginary frequencies, ensuring the presence of a minimum. The eigenvectors for each normal mode were displayed on the computer and the normal modes were assigned to specific group vibrations in a manner similar to previous vibrational frequency studies of ionic liquids.[15,16]

**Frequency Correlations.** The correlations between calculated and experimental spectra were based primarily on peak intensities and frequencies ($cm^{-1}$) for both Raman and IR.[15,16] In cases where adjacent experimental IR frequencies overlapped such that assignment was questionable, both frequencies were included in the frequency correlation diagram.

**Molecular Structures.** The gas phase molecular structures of the various gas phase conformers of $(CH_3)_3SN(CN)_2$ were determined at the B3LYP/(6-31+G(d), B3LYP/(6-311+G(d,p), B3PW91/((6-311+G(d,p), RHF/(6-311+G(d,p)), MP2/(6-311+G(d,p)), and MP3/(6-311+G(d,p)) levels of computation. The intermolecular interactions in ionic liquids include

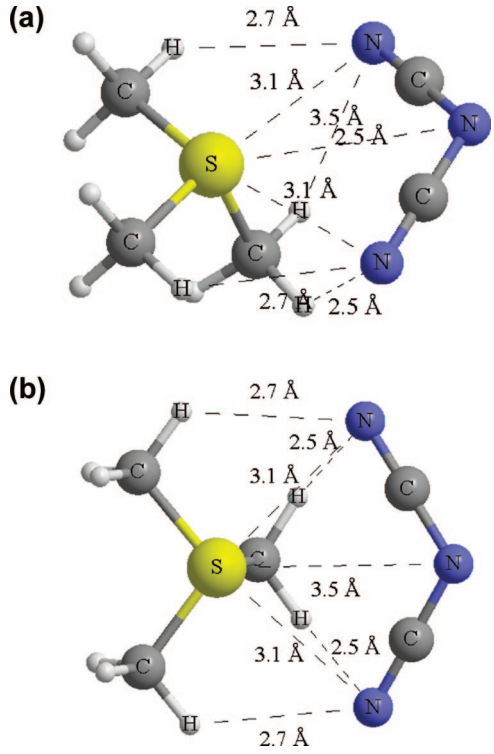


**Figure 3.** (a) $(CH_3)_3SN(CN)_2$. (b) $(CH_3)_3SN(CN)_2$ from above.

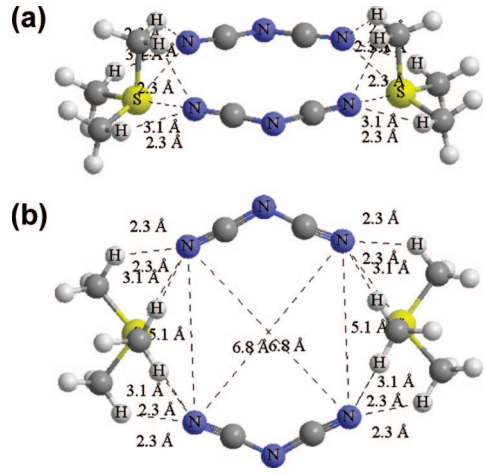


**Figure 4.** (a) $(CH_3)_3SN(CN)_2$ dimer of structural isomer 1. (b) $(CH_3)_3SN(CN)_2$ dimer of structural isomer 1, from above.

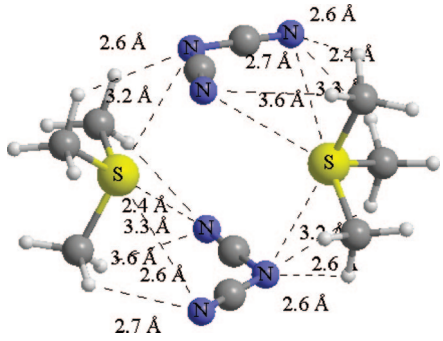


**Figure 5.** $(CH_3)_3SN(CN)_2$ of structural isomer 2, B3LYP/(6-311+G(d,p)).

dispersion forces that are not accounted for by DFT (B3LYP and B3PW91) theory. Despite this fact, DFT theory is usually quite successful in predicting accurate molecular structures and vibrational frequencies.[19−23] Previous studies have shown

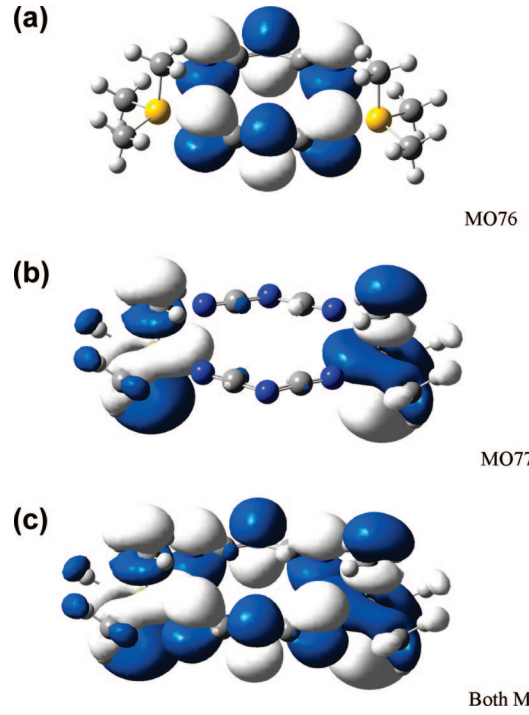


**Figure 6.** (a) $(CH_3)_3SN(CN)_2$ version 1, HOMO of B3LYP/(6-311+G(d,p)). (b) $(CH_3)_3SN(CN)_2$ version 1, LUMO of B3LYP/(6-311+G(d,p)). (c) $(CH_3)_3SN(CN)_2$ version 1, LUMO + LUMO of B3LYP/(6-311+G(d,p)).

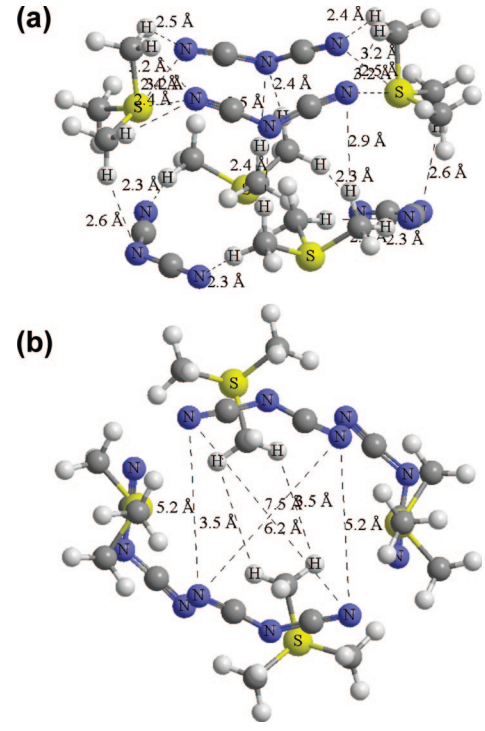


**Figure 7.** (a) Tetrameric IL resulting from combining either isomer 1 or 2, $(CH_3)_3SN(CN)_2$; B3LYP/(6-311+G(d,p)). (b) Tetrameric IL resulting from combining either isomer 1 or 2, $(CH_3)_3SN(CN)_2$, from above; B3LYP/(6-311+G(d,p)).

that DFT vibrational frequencies are generally an improvement over RHF vibrational frequencies.[15,16,24]

## Results and Discussion

**Gas Phase Structures.** Virtually identical gas phase structures were obtained for $(CH_3)_3SN(CN)_2$ using DFT,

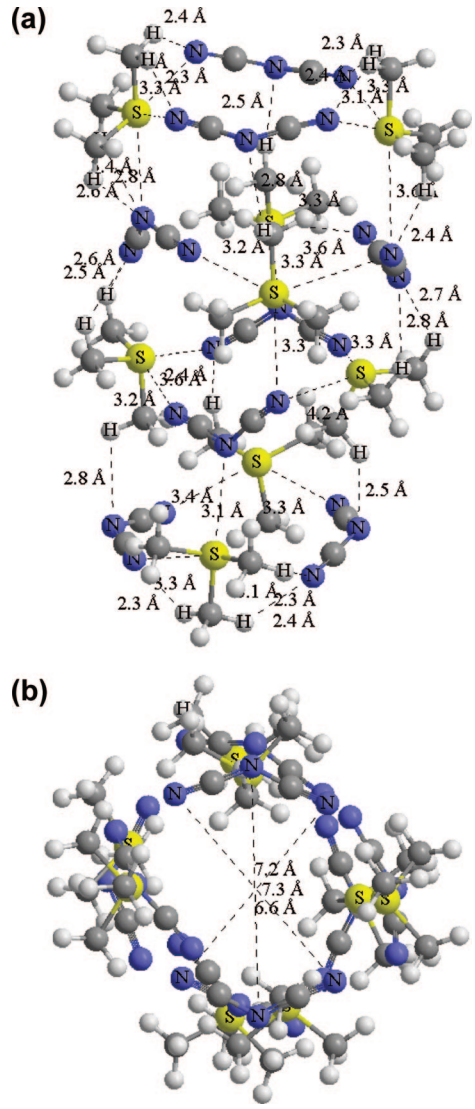


**Figure 8.** (a) Octameric IL, $(CH_3)_3SN(CN)_2$; B3LYP/(6-311+G(d,p)). (b) Octameric IL, $(CH_3)_3SN(CN)_2$, from above; B3LYP/(6-311+G(d,p)).

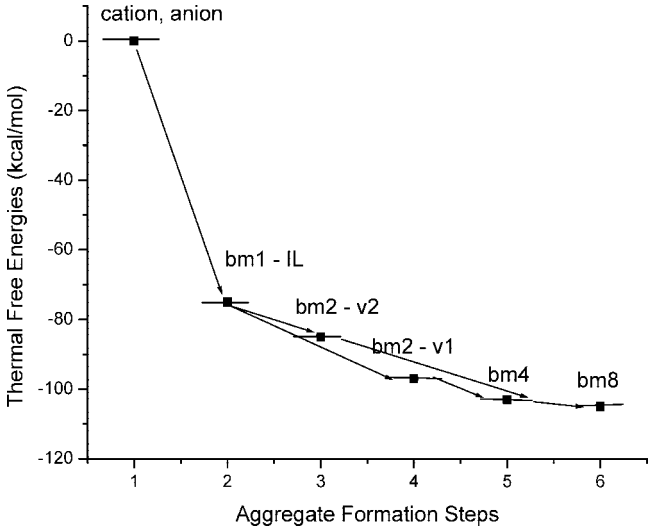


**Figure 9.** Thermal free energies of stepwise aggregate formation: bm1 = $(CH_3)_3SN(CN)_2$; bm2 = $[(CH_3)_3SN(CN)_2]_2$; bm4 = $[(CH_3)_3SN(CN)_2]_4$; bm8 = $[(CH_3)_3SN(CN)_2]_8$.

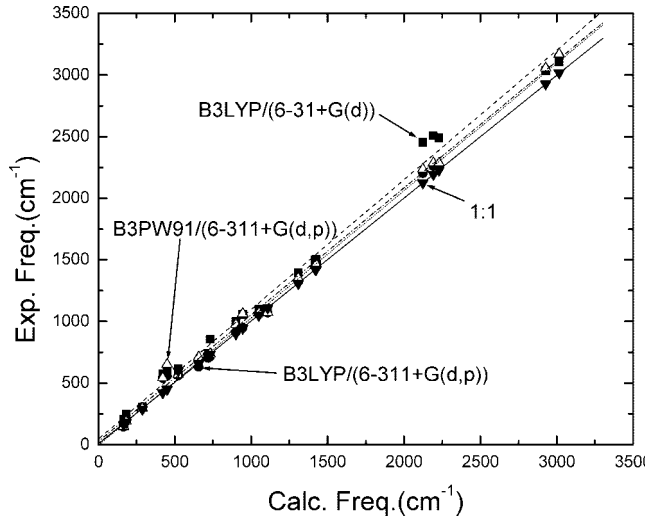


**Figure 10.** Experimental frequency ($cm^{-1}$) vs calculated frequency ($cm^{-1}$) for $(CH_3)_3SN(CN)_2$. B3LYP/(6-31+G(d)) (■) slope = 1.052; B3PW91/(6-311+G(d,p)) (Δ) slope = 1.029; B3LYP/(6-311 + G(d,p)) (●) slope = 1.033; theoretical correlation of 1.00 (▼) slope = 1.00.

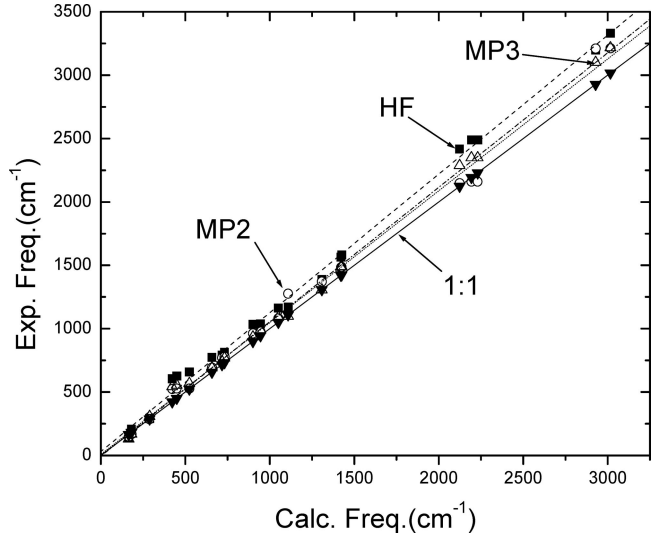


**Figure 11.** Experimental frequency ($cm^{-1}$) vs calculated frequency ($cm^{-1}$) for $(CH_3)_3SN(CN)_2$. RHF (■) slope = 1.095; MP2 (○) slope = 1.061; MP3 (Δ) slope = 1.040; theoretical correlation of 1.00 (▼) slope = 1.00. Basis set = 6-311 + G (d,p).

MP, and HF computational methods. Figure 3 shows the B3LYP/(6-311+G(d,p)) gas phase structure of $(CH_3)_3SN(CN)_2$ ionic liquid. The DFT structure of $(CH_3)_3SN(CN)_2$ in Figure 3 appears to be held together by a series of nonbonding interactions. These distances are considerably shorter than van der Waals distances (S---N distances less than 3.50 Å) including S---N distances of 3.09 Å and N---H distances of 2.28 Å. Bondi's van der Waals radii include 1.8−1.9 Å for S, 1.5 Å for N, 1.4−1.5 Å for C, and 1.1 Å for H.[25]

The $(CH_3)_3SN(CN)_2$ ionic liquid has the potential to form two distinct isomeric dimers: versions 1 and 2 (Figures 4 and 5). Version 1 is lower in free energy than version 2 by 13 kcal/mol. This is detailed in a later section.

The highest occupied (HOMO) and lowest unoccupied (LUMO) molecular orbitals of the trimethylsulfonium dicyanamide dimer, $[(CH_3)_3SN(CN)_2]_2$, are shown in Figure 6a,b. Figure

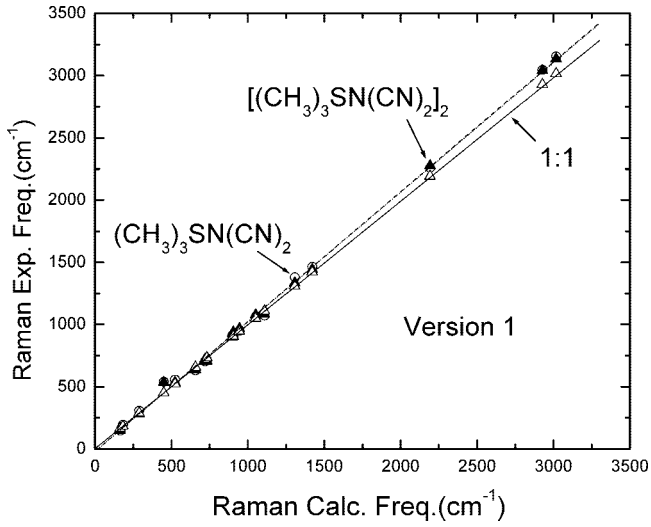


**Figure 12.** Experimental Raman frequency ($cm^{-1}$) vs calculated Raman frequency ($cm^{-1}$) for ionic liquid $(CH_3)_3SN(CN)_2$ B3LYP/(6-311+G(d,p)) (○) slope = 1.041; ionic liquid dimer $[(CH_3)_3SN(CN)_2]_2$ B3LYP/(6-311+G(d,p)) (▼) slope = 1.029; theoretical correlation of 1.00 (Δ) slope = 1.00.

6c depicts the combination of the HOMO and LUMO orbitals and displays the resulting gas phase cyclic structure of the $(CH_3)_3SN(CN)_2$ ionic liquid. The further self-aggregation of this ionic liquid will be discussed in a later section.

This is quite unlike the previously reported DFT structures for the gas phase imidazolium$-PF_6^-$ and imidazolium$-BF_4^-$ ionic liquids. In the imidazolium$-PF_6^-$ and imidazolium$-BF_4^-$ and other DFT gas phase structures, one generally observes a very short imidazolium ring C−H···F hydrogen bond that is maintained even when the ionic liquid binds to a metal surface.[7,15,16,26]

**Absolute Energies.** The B3LYP/(6-311+G(d,p)) absolute energies of $(CH_3)_3S^+$, $N(CN)_2^-$, and the ionic liquid $(CH_3)_3SN(CN)_2$ are −517.645 250, −240.563 946, and −758.328 934 au. The free energy gas phase formation of $[(CH_3)_3SN(CN)_2]$ from $(CH_3)_3S^+$ and $N(CN)_2^-$ is −75.2 kcal/mol. The two dimers of $(CH_3)_3SN(CN)_2$ (versions 1 and 2) have B3LYP/(6-311+G(d,p)) absolute energies of −1516.693 586 (version 1) and −1516.673 047 au. The free energies of formation of the two dimers are −22.4 (version 1) and −9.5 kcal/mol (version

**TABLE 1: B3LYP/(6-311+G(d,p)) Vibrational Assignments[a] ($cm^{-1}$) of $(CH_3)_3SN(CN)_2$**

| assignment[b] | $\nu$ | IR, Raman | Raman $\nu_{exp}$ | IR $\nu_{exp}$ | IR $I_{rel}$ |
|---|---|---|---|---|---|
| Cat−An tors | 54 | IR, R (w) dp | | | |
| Cat−An bend | 69 | IR, R (w) dp | | | 0.005 |
| Cat−An tors | 94 | IR | | | |
| Cat−An tors | 112 | IR, R (w) dp | | | 0.021 |
| Cat−An bend | 121 | IR, R (w) dp | | | 0.016 |
| Cat−An tors | 145 | IR, R (w) dp | 165 (0.05) | | 0.006 |
| S−Me twist | 193 | IR, R (m) p | 182 (0.60) | | 0.055 |
| S−Me twist | 210 | IR | | | |
| S−Me twist | 226 | IR | | | |
| S−Me twist | 254 | IR, R (w) dp | | | |
| S−Me twist | 268 | IR, R (w) dp | | | |
| S−Me twist | 280 | IR, R (w) dp | | | |
| C−S bend | 306 | IR, R (w) dp | 288 (0.22) | | |
| N−C−N bend | 540 | IR, R (w) dp | 422 (0.06) | | 0.014 |
| N−C−N bend | 557 | IR, R (w) dp | 450 (0.15) | | |
| N−C−N bend | 561 | IR | | 524 (0.022) | 0.028 |
| sym C−S str | 631 | IR, R (m) p | 657 (0.93) | 655 (0.008) | 0.002 |
| sym C−S str, C−N bend | 702 | IR, R (m) p | 720 (0.20) | | 0.004 |
| asym C−S str | 714 | IR, R (m) dp | 732 (0.33) | | |
| sym C−N−C bend | 720 | IR, R (w) p | | | 0.01 |
| H−C−H bend | 913 | IR, R (w) dp | 900 (0.09) | 905 (0.011) | 0.012 |
| H−C−H bend | 949 | IR, R (w) dp | | 945 (0.007) | 0.026 |
| C−N−C sym str, H−C−H bend | 950 | IR, R (w) p | | | 0.012 |
| C−N−C sym str, H−C−H bend | 958 | IR, R (w) p | | | 0.018 |
| H−C−H bend | 1061 | IR, R (w) p | 1051 (0.07) | 1050 (0.037) | 0.036 |
| H−C−H bend, C−S sym str | 1071 | IR, R (w) p | 1109 (0.05) | | 0.045 |
| H−C−H bend, C−S asym str | 1072 | IR, R (w) dp | | | 0.011 |
| asym C−N−C str, H−C−H bend | 1322 | IR | | 1308 (0.060) | 0.131 |
| H−C−H bend | 1340 | IR | | | 0.006 |
| asym C−N−C str, H−C−H bend | 1345 | IR | | | |
| H−C−H bend | 1379 | IR, R (w) p | | | 0.026 |
| methyl wag | 1443 | IR, R (w) dp | | | |
| methyl wag | 1463 | IR, R (w) dp | | | 0.032 |
| methyl wag | 1464 | IR, R (m) p | 1421 (0.16) | | 0.003 |
| methyl wag | 1472 | IR, R (m) dp | 1421 (0.16) | | 0.007 |
| methyl wag | 1478 | IR, R (w) p | | 1426 (0.030) | 0.023 |
| methyl wag | 1499 | IR, R (w) dp | | | 0.035 |
| N−C−N asym str | 2203 | IR, R (w) p | | 2124 (1.00) | 1 |
| N−C−N sym str | 2259 | IR, R (vs) p | 2193 (0.96) | 2230 (0.480) | 0.275 |
| H−C−H sym str | 3047 | IR, R (vs) p | 2928 (1.00) | | 0.027 |
| H−C−H sym str | 3049 | IR, R (vs) p | | 2929 (0.013) | 0.018 |
| H−C−H sym str | 3049 | IR, R (w) p | | | 0.002 |
| H−C−H asym str | 3148 | IR, R (m) dp | | 3016 (0.051) | 0.007 |
| H−C−H asym str | 3148 | IR, R (s) p | | | 0.005 |
| H−C−H asym str | 3154 | IR, R (vs) dp | 3017 (0.24) | | 0.003 |
| H−C−H asym str | 3155 | IR, R (m) dp | | | 0.002 |
| H−C−H asym str | 3156 | IR, R (m) p | | | 0.002 |
| H−C−H asym str | 3159 | IR, R (m) dp | | | 0.012 |

[a] Note that experimental and calculated (IR) spectra are normalized to the most intense absorbance peak. Theoretical Raman spectra: vs = 0.5−1.0, s = 0.25−0.5, m = 0.05−0.25, w < 0.05. [b] Cat = cation; An = anion.

**TABLE 2: B3PW91/(6-311+G(d,p)) Vibrational Assignments[a] ($cm^{-1}$) of $(CH_3)_3SN(CN)_2$**

| assignment[b] | $\nu$ | IR, Raman | Raman $\nu_{exp}$ | IR $\nu_{exp}$ | IR $I_{rel}$ |
|---|---|---|---|---|---|
| Cat−An tors | 54 | IR, R (w) dp | | | |
| Cat−An tors | 69 | IR, R (w) dp | | | 0.006 |
| Cat−An tors | 92 | IR | | | |
| Cat−An tors | 111 | IR | | | 0.026 |
| Cat−An tors | 123 | IR | | | 0.022 |
| Cat−An bend | 147 | IR, R (w) dp | 165 (0.05) | | 0.007 |
| S−Me twist | 191 | IR, R (m) p | 182 (0.60) | | 0.072 |
| N−C−N bend | 204 | IR | | | |
| S−Me twist | 223 | IR | | | |
| C−S−C bend | 253 | IR, R (w) dp | | | |
| S−Me twist | 259 | IR, R (w) dp | | | |
| S−Me twist | 273 | IR, R (w) dp | | | |
| C−S−C bend | 295 | IR, R (w) dp | 288 (0.22) | | |
| N−C−N bend | 541 | IR, R (w) p | 422 (0.06) | | 0.016 |
| N−C−N bend | 557 | IR | | | |
| 1-C−N bend | 568 | IR | | 524 (0.022) | 0.029 |
| sym C−S str | 651 | IR, R (m) p | 450 (0.15) | | 0.002 |
| C−N sym bend | 711 | IR, R (w) p | 657 (0.93) | 655 (0.008) | 0.016 |
| sym C−S str, C−N sym bend | 727 | IR, R (w) dp | 720 (0.20) | | |
| C−S asym str | 736 | IR, R (m)dp | 732 (0.33) | | 0.001 |
| H−C−H bend | 912 | IR, R (w) p | | | |
| H−C−H bend | 947 | IR, R (w) dp | | | |
| H−C−H bend | 953 | IR, R (w) p | | | 0.006 |
| H−C−H bend, C−N sym str | 974 | IR, R (w) p | 900 (0.09) | 905 (0.011) | 0.031 |
| H−C−H bend | 1064 | IR, R (w) dp | | 945 (0.007) | 0.046 |
| H−C−H bend | 1070 | IR, R (w) dp | 1051 (0.07) | 1050 (0.037) | 0.047 |
| H−C−H bend | 1074 | IR, R (w) p | 1109 (0.05) | | 0.015 |
| asym C−N−C str, methyl wag | 1334 | IR | | | 0.091 |
| methyl wag | 1336 | IR, R (w) p | | | 0.007 |
| C−N−C asym str, H−C−H bend | 1352 | IR | | 1308 (0.060) | 0.063 |
| H−C−H bend | 1375 | IR, R (w) dp | | | 0.036 |
| H−C−H bend | 1430 | IR, R (w) p | | | |
| H−C−H bend | 1452 | IR, R (w) p | | | 0.033 |
| H−C−H bend | 1454 | IR, R (m) dp | 1421 (0.16) | | 0.002 |
| H−C−H bend | 1463 | IR, R (m) dp | | 1426 (0.030) | 0.017 |
| H−C−H bend | 1467 | IR, R (w) p | | | 0.003 |
| H−C−H bend | 1486 | IR, R (w) p | | | 0.035 |
| N−C−N asym str | 2236 | IR, R (w) dp | | 2124 (1.00) | 1 |
| N−C−N sym str | 2286 | IR, R(vs) p | 2193 (0.96) | 2230 (0.480) | 0.316 |
| H−C−H sym str | 3052 | IR, R(vs) p | | | 0.034 |
| H−C−H sym str | 3055 | IR, R(vs) p | 2928 (1.00) | 2929 (0.013) | 0.02 |
| H−C−H sym str | 3055 | IR, R (w) p | | | 0.001 |
| H−C−H asym str | 3162 | IR, R (m) dp | | | 0.01 |
| H−C−H asym str | 3163 | IR, R (s) p | | | 0.008 |
| H−C−H asym str | 3168 | IR, R (m) dp | 3017 (0.24) | 3016 (0.051) | 0.015 |
| H−C−H asym str | 3171 | IR, R (vs) dp | 3017 (0.24) | | 0.002 |
| H−C−H asym str | 3173 | IR, R (vs) dp | | | 0.001 |
| H−C−H asym str | 3173 | IR, R (m) dp | | | 0.002 |

[a] Note that experimental and calculated (IR) spectra are normalized to the most intense absorbance peak. Theoretical Raman spectra: vs = 0.5−1.0, s = 0.25−0.5, m = 0.05−0.25, w < 0.05. [b] Cat = cation; An = anion.

2). The combination of either one of these two dimers to form an ionic liquid tetramer results in the same structure (Figure 7) whose absolute energy is −3033.395 503 au. The octamer of $(CH_3)_3SN(CN)_2$ shown in Figure 8 has an absolute energy of −6066.793 295 au. Figure 9 is a schematic outline of the various gas phase steps and thermal free energies that may occur from the initial formation of $(CH_3)_3SN(CN)_2$ to the final octameric structure, $[(CH_3)_3SN(CN)_2]_8$.

The steps outlined in Figure 9 indicate highly exergonic driving forces that lead to a series of $[(CH_3)_3SN(CN)_2]_n$ ($n$ = 1, 2, 4, 8) cyclic structures. This initial reaction of the cationic and anionic salts of $(CH_3)_3SN(CN)_2$ is strong enough (−75.2 kcal/mol) to ensure its rapid and relatively complete formation. Any additional steps that potentially may occur are driven by exergonic forces leading to the formation of these unusual aggregates.

**TABLE 3: B3LYP/(6-31+G(d)) Vibrational Assignments[a] ($cm^{-1}$) of $(CH_3)_3SN(CN)_2$**

| assignment[b] | $\nu$ | IR, Raman | Raman $\nu_{exp}$ | IR $\nu_{exp}$ | IR $I_{rel}$ |
|---|---|---|---|---|---|
| Cat−An tors | 59 | IR, R (w) dp | | | 0.006 |
| Cat−An bend | 64 | IR | | | |
| Cat−An tors | 87 | IR, R (w) p | | | 0.005 |
| Cat−An bend | 204 | IR, R (w) dp | 165 (0.05) | | 0.02 |
| Cat−An tors, S−Me bend | 251 | IR, R (w) p | 182 (0.60) | | 0.002 |
| Cat−An bend, C−S bend | 255 | IR, R (w) dp | | | 0.002 |
| Cat−An bend, C−S bend | 278 | IR, R (w) dp | | | 0.002 |
| C−S bend, Cat−An bend | 304 | IR, R (w) p | 288 (0.22) | | 0.011 |
| C−S bend | 328 | IR | | | |
| C−S bend | 356 | IR | | | |
| S−Me twist and bend | 367 | IR, R (w) dp | | | |
| S−Me twist and bend | 391 | IR | | | |
| S−Me twist and bend | 407 | IR, R (m)dp | | | 0.041 |
| N−C−N bend | 574 | IR, R (m)dp | 422 (0.06) | | 0.009 |
| N−C−N bend | 602 | IR, R (w) p | 450 (0.15) | | 0.001 |
| C−N bend | 615 | IR | | 524 (0.022) | |
| N−C−N bend | 627 | IR, R (w) p | | | 0.004 |
| N−C−N bend | 640 | IR | | | 0.009 |
| asym C−S str | 656 | IR, R (m) dp | 657 (0.93) | 655 (0.008) | 0.002 |
| asym C−N−C str | 743 | IR, R (m) dp | 720 (0.20) | | 0.002 |
| H−C−S bend | 856 | IR, R (w) dp | 732 (0.33) | | 0.009 |
| H−C−H bend | 982 | IR, R (w) p | | | 0.001 |
| H−C−H bend, C−N−C sym str | 1001 | IR, R (w) p | 900 (0.09) | 905 (0.011) | |
| H−C−H bend, C−N−C sym str | 1016 | IR, R (w) dp | | | 0.001 |
| H−C−H bend | 1056 | IR, R (w) dp | | 945 (0.007) | 0.034 |
| H−C−H bend, C−S bend | 1098 | IR, R (w) dp | 1051 (0.07) | 1050 (0.037) | 0.008 |
| H−C−H bend, C−S str | 1103 | IR, R (w) dp | | | 0.003 |
| asym C−N−C str | 1108 | IR, R (w) p | 1109 (0.05) | | 0.002 |
| H−C−H sym bend, C−S str | 1394 | IR, R (w) p | | 1308 (0.060) | 0.002 |
| H−C−H sym bend, C−S str | 1425 | IR, R (w) dp | | | |
| H−C−H sym bend, C−S str | 1456 | IR, R (w) p | | | 0.009 |
| H−C−H bend | 1466 | IR, R (w) dp | | | 0.003 |
| H−C−H bend | 1482 | IR, R (m) dp | | | 0.001 |
| H−C−H bend | 1499 | IR, R (m) p | 1421 (0.16) | 1426 (0.030) | 0.003 |
| H−C−H bend | 1503 | IR,R (m) dp | | | 0.001 |
| H−C−H bend | 1513 | IR, R (w) dp | | | 0.015 |
| H−C−H bend | 1526 | IR, R (w) p | | | 0.009 |
| N−C−N asym str | 1935 | IR, R (m) dp | | | 0.254 |
| N−C−N sym str | 2008 | IR, R (vs) p | | | 0.092 |
| H−C−H sym str | 2454 | IR, R (w) dp | | 2124 (1.00) | 0.005 |
| H−C−H sym str | 2506 | IR, R (vs) p | 2193 (0.96) | 2230 (0.480) | 1 |
| H−C−H sym str | 3009 | IR, R (vs) p | | | 0.001 |
| H−C−H asym str | 3036 | IR, R (vs) p | 2928 (1.00) | 2929 (0.013) | 0.006 |
| H−C−H asym str | 3038 | IR, R (m) dp | | | 0.002 |
| H−C−H asym str | 3104 | IR, R (w) dp | | | |
| H−C−H asym str | 3105 | IR, R (vs) p | 3017 (0.24) | 3016 (0.051) | 0.002 |
| H−C−H asym str | 3105 | IR, R (m) p | | | |
| H−C−H asym str | 3109 | IR, R (s) dp | | | |

[a] Note that experimental and calculated (IR) spectra are normalized to the most intense absorbance peak. Theoretical Raman spectra: vs = 0.5−1.0, s = 0.25−0.5, m = 0.05−0.25, w < 0.05. [b] Cat = cation; An = anion.

**Raman Spectra and Correlation Diagrams. *$(CH_3)_3SN(CN)_2$: B3LYP and B3PW91.*** Tables 1, 2, and 3 contain the Raman and IR theoretical and experimental vibrations for the $(CH_3)_3SN(CN)_2$ ionic liquid. The theoretical and experimental vibrational bands correlate well for the B3LYP and B3PW91 methods using the 6-311+G(d,p) basis set as shown in Figure 10. The slopes of the B3LYP/(6-311+G(d,p)) and B3PW91/(6-311+G(d,p)) results shown in Figure 10 correspond (inverse relationship) to a scale factor of 0.97 with a correlation coefficient ($R^2$) of 0.998. Use of the 6-31+G(d) basis set with B3LYP (Table 3) lowers the scale factor to 0.95 and the correlation coefficient ($R^2$) to 0.992. Similar results were reported for imidazolium−$PF_6^-$ and imidazolium−$BF_4^-$ ionic liquids.[15,16]

As indicated in Tables 1 and 2, the strongest Raman band at 288 $cm^{-1}$ is assigned to the S−$CH_3$ twist. The Raman vibrations in the 657−732 $cm^{-1}$ region can be associated with C−S bond bend and stretches (B3LYP, Table 1) or a combination of C−S and C−N bend and stretch vibrations (B3PW91, Table 2). The Raman band at 1421 $cm^{-1}$ is assigned to a methyl wag vibration. The strong Raman band

**TABLE 4: MP2/(6-311+G(d,p)) Vibrational Assignments[a] ($cm^{-1}$) of $(CH_3)_3SN(CN)_2$**

| assignment[b] | $\nu$ | IR, Raman | Raman $\nu_{exp}$ | IR $\nu_{exp}$ | IR $I_{rel}$ |
|---|---|---|---|---|---|
| Cat−An tors | 59 | IR, R (w) dp | | | 0.006 |
| Cat−An tors | 73 | IR, R (w) dp | | | |
| Cat−An tors | 101 | IR | | | |
| Cat−An bend | 120 | IR, R (m) dp | | | 0.022 |
| Cat−An bend | 130 | IR, R (m) dp | | | 0.026 |
| Cat−An bend | 148 | IR, R (w) dp | 165 (0.05) | | 0.006 |
| S−Me twist | 168 | IR, R (m) p | 182 (0.60) | | 0.087 |
| N−C−N sym bend | 199 | IR | | | |
| S−Me twist | 226 | IR | | | |
| S−Me twist | 242 | IR | | | |
| S−Me twist | 264 | IR, R (w) dp | | | |
| S−Me twist | 286 | IR, R (w) dp | 288 (0.22) | | |
| C−S−C bend | 307 | IR | | | |
| N−C−N asym bend | 521 | IR | | | 0.018 |
| N−C−N asym bend | 525 | IR, R (w) p | 422 (0.06) | | 0.023 |
| N−C−N sym bend | 529 | IR, R (w) p | 450 (0.15) | 524 (0.022) | |
| C−S sym str | 693 | IR, R (s) p | 657 (0.93) | | 0.002 |
| C−N−C sym bend | 697 | IR, R (w) p | | 655 (0.008) | 0.009 |
| C−S str | 770 | IR, R (m) dp | 717 (0.20) | | 0.002 |
| C−S asym str | 778 | IR, R (m) dp | 732 (0.33) | | |
| H−C−H bend | 926 | IR | | | |
| C−N−C sym str | 963 | IR, R (m) p | 900 (0.09) | 905 (0.011) | 0.033 |
| H−C−H bend | 968 | IR, R (w) dp | | | |
| H−C−H bend | 976 | IR | | 945 (0.007) | 0.002 |
| H−C−H bend | 1081 | IR, R (w) p | 1051 (0.07) | 1050 (0.037) | 0.056 |
| H−C−H bend | 1088 | IR, R (w) dp | | | 0.012 |
| H−C−H bend | 1088 | IR, R (w) p | | | 0.037 |
| C−N−C asym str | 1276 | IR, R (w) p | 1109 (0.05) | | 0.172 |
| methyl wag | 1367 | IR | | | 0.007 |
| methyl wag | 1372 | IR | | 1308 (0.060) | 0.006 |
| methyl wag | 1410 | IR, R (w) p | | | 0.04 |
| H−C−H bend | 1454 | IR, R (w) dp | | | |
| H−C−H bend | 1477 | IR, R (m) dp | | | |
| H−C−H bend | 1480 | IR, R (w) dp | | | 0.048 |
| H−C−H bend | 1482 | IR, R (m) dp | 1421 (0.16) | | 0.004 |
| H−C−H bend | 1487 | IR, R (w) p | | 1426 (0.030) | 0.024 |
| H−C−H bend | 1504 | IR, R (w) dp | | | 0.04 |
| N−C−N asym str | 2148 | IR, R (m) dp | | 2124 (1.00) | 1 |
| N−C−N sym str | 2159 | IR, R (vs) p | 2193 (0.96) | 2230 (0.480) | 0.255 |
| H−C−H sym str | 3087 | IR, R (vs) p | | | 0.052 |
| H−C−H sym str | 3088 | IR, R (vs) p | | | 0.005 |
| H−C−H sym str | 3089 | IR, R (w) dp | | | 0.002 |
| H−C−H asym str | 3207 | IR, R (vs) p | | | 0.01 |
| H−C−H asym str | 3207 | IR, R (s) dp | | | 0.015 |
| H−C−H asym str | 3211 | IR, R (vs) dp | 2928 (1.00) | 2929 (0.013) | 0.003 |
| H−C−H asym str | 3212 | IR, R (vs) dp | | | 0.002 |
| H−C−H asym str | 3212 | IR, R (m) dp | | | |
| H−C−H asym str | 3212 | IR, R (s) dp | 3017 (0.24) | 3016 (0.051) | 0.021 |

[a] Note that experimental and calculated (IR) spectra are normalized to the most intense absorbance peak. Theoretical Raman spectra: vs = 0.5−1.0, s = 0.25−0.5, m = 0.05−0.25, w < 0.05. [b] Cat = cation; An = anion.

at 2193 $cm^{-1}$ is assigned to an N−C−N symmetric stretch, and the vibrations at 2928 and 3017 $cm^{-1}$ are associated with H−C−H symmetric stretch vibrations.

***$(CH_3)_3SN(CN)_2$: MP2, MP3, and RHF.*** Tables 4, 5, and 6 contains Møller−Plesset[27] (MP2 and MP3) and RHF results using the 6-311+G(d,p) basis set under tight fit requirements. The results and assignments are virtually identical to those obtained using the B3LYP and B3PW91 methods (Tables 1 and 2). These data are plotted in Figure 11. In Figure 11, the results improve from RHF to MP2 to MP3 with the slopes decreasing from 1.095 to 1.061 to 1.040. The slopes are representative of scale factors of 0.913 (HF), 0.943 (MP2), and 0.962 (MP3).

***$(CH_3)_3SN(CN)_2$: Monomer and Dimer.*** Figure 12 contains a comparison between calculated B3LYP and experimental Raman vibrations for $(CH_3)_3SN(CN)_2$ and its version 1 (lowest energy form) dimer, $[(CH_3)_3SN(CN)_2]_2$, using the 6-311+G(d,p) basis set. As one increases the number of ionic liquids in the aggregate forms (dimer, tetramer, octamer), the number of calculated Raman vibrations increases accordingly; however, the differences in their energies serve to shift the Raman frequencies only slightly. In Figure 12 the

**TABLE 5: MP3/(6-311+G(d,p)) Vibrational Assignments[a] ($cm^{-1}$) of $(CH_3)_3SN(CN)_2$**

| assignment[b] | $\nu$ | IR, Raman | Raman $\nu_{exp}$ | IR $\nu_{exp}$ | IR $I_{rel}$ |
|---|---|---|---|---|---|
| Cat−An tors | 57 | IR | | | |
| Cat−An tors | 57 | IR | | | |
| Cat−An tors | 97 | IR | | | 0.02 |
| Cat−An tors | 117 | IR | | | 0.009 |
| Cat−An bend | 129 | IR, R (w) dp | 165 (0.05) | | 0.017 |
| Cat−An tors | 148 | IR | | | 0.008 |
| Cat−An bend | 168 | IR, R (m) p | 182 (0.60) | | 0.04 |
| C−S bend | 203 | IR, R (w) dp | | | |
| Me twist | 220 | IR, R (w) dp | | | |
| Me twist | 240 | IR, R (w) p | | | |
| S−Me twist | 265 | IR | | | 0.001 |
| S−Me twist | 286 | IR | | | |
| S−Me bend | 307 | IR, R (w) p | 288 (0.22) | | 0.041 |
| N−C−N bend | 542 | IR, R (w) dp | 422 (0.06) | | 0.017 |
| C−N bend | 553 | IR, R (m) p | 450 (0.15) | | 0.006 |
| C−N bend | 567 | IR, R (w) dp | | 524 (0.022) | |
| N−C−N asym str and bend | 691 | IR, R (w) p | 657 (0.93) | 655 (0.008) | 0.043 |
| sym C−S str | 742 | IR, R (m) p | 717 (0.20) | | 0.004 |
| asym C−S str | 768 | IR, R (m) dp | 732 (0.33) | | |
| asym C−N−C bend and str | 779 | IR, R (w) p | | | 0.006 |
| sym C−N−C bend and str | 936 | IR, R (w) p | 900 (0.09) | 905 (0.011) | 0.044 |
| Me twist | 976 | IR | | | |
| H−C−H bend | 982 | IR, R (w) dp | | | |
| C−N bend | 989 | IR | | 945 (0.007) | 0.001 |
| H−C−H bend | 1089 | IR, R (w) p | 1051 (0.07) | 1050 (0.037) | 0.026 |
| H−C−H bend, C−S str | 1098 | IR, R (w) p | | | 0.024 |
| H−C−H bend, C−S str | 1098 | IR, R (w) dp | 1109 (0.05) | | 0.007 |
| asym C−N−C str | 1307 | IR | | 1308 (0.060) | 0.174 |
| H−C−H sym bend | 1385 | IR, R (w) dp | | | 0.005 |
| H−C−H sym bend | 1389 | IR, R (w) dp | | | |
| H−C−H sym bend, C−S str | 1427 | IR, R (w) p | | | 0.018 |
| H−C−H bend | 1465 | IR, R (w) dp | | | |
| H−C−H sym bend | 1486 | IR, R (m) dp | 1421 (0.16) | | |
| H−C−H bend | 1489 | IR, R (w) dp | | 1426 (0.030) | 0.031 |
| H−C−H bend | 1490 | IR, R (m) dp | | | 0.002 |
| H−C−H bend | 1495 | IR, R (w) dp | | | 0.019 |
| H−C−H bend | 1512 | IR, R (w) dp | | | 0.025 |
| N−C−N asym str | 2287 | IR, R (m) dp | | 2124 (1.00) | 1 |
| N−C−N sym str | 2348 | IR, R (vs) p | 2193 (0.96) | 2230 (0.480) | 0.284 |
| H−C−H sym str | 3101 | IR, R (w) dp | | | |
| H−C−H sym str | 3101 | IR, R (vs) p | 2928 (1.00) | 2929 (0.013) | 0.008 |
| H−C−H sym str | 3103 | IR, R (vs) p | | | 0.038 |
| H−C−H asym str | 3210 | IR, R (m) dp | | | 0.002 |
| H−C−H asym str | 3211 | IR, R (vs) dp | | | 0.004 |
| H−C−H asym str | 3212 | IR, R (m) dp | | | 0.005 |
| H−C−H asym str | 3212 | IR, R (s) dp | | | 0.002 |
| H−C−H sym and asym str | 3217 | IR, R (vs) dp | 3017 (0.24) | 3016 (0.051) | 0.002 |
| H−C−H asym str | 3226 | IR, R (s) dp | | | 0.009 |

[a] Note that experimental and calculated (IR) spectra are normalized to the most intense absorbance peak. Theoretical Raman spectra: vs = 0.5−1.0, s = 0.25−0.5, m = 0.05−0.25, w < 0.05. [b] Cat = cation; An = anion.

theoretical slopes of the monomer and dimer forms of $(CH_3)_3SN(CN)_2$ are virtually identical (slope = 1.03, scale factor = 0.97, correlation coefficient = 0.998). It is apparent that the potential aggregation process for the $(CH_3)_3SN(CN)_2$ ionic liquid has little effect on the calculated Raman spectrum.

## Conclusions

The possible formation of $(CH_3)_3SN(CN)_2$ ionic liquid aggregates is supported by vibrational spectra (Raman and IR) and theoretical calculations using various ab initio and DFT methods. Theoretical results suggest that $(CH_3)_3SN(CN)_2$ forms a cyclic dimer that may further undergo a "stacking" process, resulting in the formation of tetramers and octamers. It is also conceivable that more complex structures are formed as the process of aggregation occurs. The unusual cyclic structure of $[(CH_3)_3SN(CN)_2]_2$ may be capable of forming ionic liquid nanotubes. In view of the vast number of ionic liquids,[28] it is only a matter of time before other potential ionic liquid nanotubes are pointed out by various investigators.

**TABLE 6: HF/(6-311+G(d,p)) Vibrational Assignments[a] ($cm^{-1}$) of $(CH_3)_3SN(CN)_2$**

| assignment[b] | $\nu$ | IR, Raman | Raman $\nu_{exp}$ | IR $\nu_{exp}$ | IR $I_{rel}$ |
|---|---|---|---|---|---|
| Cat−An tors | 20 | IR | | | |
| Cat−An bend | 65 | IR, R (w) dp | | | 0.004 |
| Cat−An bend | 88 | IR | | | |
| Cat−An tors | 103 | IR | | | 0.022 |
| Cat−An bend | 121 | IR | | | 0.014 |
| Cat−An tors | 143 | IR, R (w) dp | 165 (0.05) | | 0.013 |
| S−Me twist | 207 | IR, R (m) p | 182 (0.60) | | 0.038 |
| N−C−N sym bend | 208 | IR | | | |
| S−Me twist | 233 | IR | | | |
| S−Me twist | 261 | IR | | | |
| C−S−C sym bend | 275 | IR, R (w) dp | | | |
| C−S−C asym bend | 291 | IR, R (w) dp | 288 (0.22) | | |
| C−S−C sym bend | 315 | IR | | | |
| N−C−N asym bend | 605 | IR, R (w) p | 422 (0.06) | | 0.018 |
| N−C−N asym bend | 627 | IR, R (w) dp | 450 (0.15) | | |
| N−C−N sym bend | 660 | IR | | 524 (0.122) | 0.045 |
| sym C−S str | 680 | IR, R (m) p | | | 0.003 |
| asym C−S str | 775 | IR, R (m) p | 657 (0.931) | 655 (0.021) | 0.003 |
| asym C−S str | 793 | IR, R (m) dp | 717 (0.20) | | 0.001 |
| sym C−N−C bend | 814 | IR, R (w) dp | 732 (0.33) | | 0.01 |
| Me twist | 1001 | IR, R (w) p | | | |
| C−N−C sym str | 1034 | IR, R (w) p | 900 (0.09) | 905 (0.16) | 0.041 |
| H−C−H bend | 1039 | IR, R (w) dp | | 945 (0.10) | |
| H−C−H bend | 1046 | IR | | | |
| H−C−H bend | 1164 | IR, R (w) dp | 1051 (0.07) | 1050 (0.48) | 0.024 |
| H−C−H bend | 1171 | IR, R (w) p | 1109 (0.05) | | 0.022 |
| H−C−H bend | 1174 | IR, R (w) dp | | | 0.01 |
| asym C−N−C str | 1387 | IR | | 1308 (0.55) | 0.18 |
| H−C−H sym bend | 1477 | IR, R (w) p | | | 0.005 |
| H−C−H sym bend | 1479 | IR, R (w) dp | | | |
| H−C−H sym bend | 1518 | IR, R (w) p | | | 0.013 |
| H−C−H asym bend | 1565 | IR, R (w) dp | 1421 (0.16) | | |
| H−C−H sym bend | 1583 | IR | | 1426 (0.42) | 0.028 |
| H−C−H asym bend | 1584 | IR, R (m) dp | | | |
| H−C−H asym bend | 1587 | IR, R (m) dp | | | |
| H−C−H asym bend | 1594 | IR | | | 0.019 |
| H−C−H sym bend | 1612 | IR, R (w) p | | | 0.03 |
| N−C−N asym str | 2418 | IR, R (m) dp | | 2124 (1.00) | 1 |
| N−C−N sym str | 2489 | IR, R (vs) p | 2193 (0.96) | 2230 (0.480) | 0.28 |
| H−C−H asym str | 3197 | IR, R (w) dp | | | |
| H−C−H sym str | 3199 | IR, R (vs) p | 2928 (1.00) | 2924 (0.23) | 0.014 |
| H−C−H sym str | 3203 | IR, R (vs) p | 2928 (1.00) | | 0.022 |
| H−C−H asym str | 3301 | IR, R (m) dp | | | |
| H−C−H asym str | 3302 | IR, R (vs) dp | | | 0.005 |
| H−C−H asym str | 3307 | IR, R (m) dp | | | 0.007 |
| H−C−H asym str | 3307 | IR, R (s) dp | | | |
| H−C−H asym str | 3314 | IR, R (s) dp | | | 0.003 |
| H−C−H asym str | 3331 | IR, R (s) dp | 3017 (0.24) | 3016 (0.48) | 0.009 |

[a] Note that experimental and calculated (IR) spectra are normalized to the most intense absorbance peak. Theoretical Raman spectra: vs = 0.5−1.0, s = 0.25−0.5, m = 0.05−0.25, w < 0.05. [b] Cat = cation; An = anion.

**Acknowledgment.** The authors wish to acknowledge financial support from the Air Force Office of Scientific Research via Contract No. FA9550-05-C-0182 (W.R.C.). This work was initiated during a Mercator Visiting Professorship (W.R.C.) at RWTH, Aachen, Germany

## References and Notes

(1) Wasserscheid, P.; Keim, W. *Angew. Chem., Int. Ed.* **2000**, *39*, 3772–3789.

(2) Welton, T. *Chem. Rev.* **1999**, *99*, 2071–2083.

(3) Wilkes, J. S. *Green Chem.* **2002**, *4*, 73–80.

(4) *Ionic Liquids in Synthesis*, 2nd ed.; Wasserscheid, P., Welton, T., Eds.; John Wiley: New York, 2008; Vols. *1 & 2*.

(5) Earle, M. J.; McCormac, P. B.; Seddon, K. R. *Green Chem.* **1999**, *1*, 23–25.

(6) Schulz, P. S.; Müller, N.; Bösmann, A.; Wasserscheid, P. *Angew. Chem., Int. Ed.* **2007**, *46*, 1293–1295.

(7) Nooruddin, N. S.; Wahlbeck, P. G.; Carper, W. R. *J. Mol. Struct. (THEOCHEM)* **2007**, *822*, 1–7.

(8) Gerhard, D.; Alpasian, S. C.; Gores, H. J.; Uerdingen, M.; Wasserscheid, P. *Chem. Commun.* **2005**, 5080–5082.

(9) Dorbritz, S.; Ruth, W.; Kragl, U. *Adv. Synth. Catal.* **2005**, *347*, 1273–1279.

(10) Bini, R.; Bortolini, O.; Chiappe, C.; Pieraccini, D.; Siciliano, T. *J. Phys. Chem. B* **2007**, *111*, 598–604.

(11) Modaressi, A.; Sifaoui, H.; Mielcarz, M.; Domanska, U.; Rogalski, M. *Colloids Surf., A: Physicochem. Eng. Aspects* **2007**, *302*, 181–185.

(12) Strasser, D.; Goulay, F.; Kelkar, M. S.; Maginn, E. J.; Leone, S. R. *J. Phys. Chem. A* **2007**, *111*, 3191–3195.
(13) Berg, R. W. *Monatsh. Chem.* **2007**, *135*, 1045–1075.
(14) Iwata, K.; Okajima, H.; Saha, S.; Hamaguchi, H. *Acc. Chem. Res.* **2007**, *40*, 1174–1181.
(15) Talaty, E. A.; Raja, S.; Storhaug, V. J.; Dolle, S.; Carper, W. R. *J. Phys. Chem. B* **2004**, *108*, 13177–13184.
(16) Heimer, N. E.; Del Sesto, R. E.; Meng, Z.; Wilkes, J. S.; Carper, W. R. *J. Mol. Liq.* **2006**, *124*, 84–95.
(17) Paulsson, H.; Berggrund, M.; Svantesson, E.; Hagfeldt, A.; Kloo, L. *Sol. Energy Mater. Sol. Cells* **2004**, *82*, 345–360.
(18) Frisch, M. J.; Trucks, G. W.; Schlegel, H. B.; Scuseria, G. E.; Robb, M. A.; Cheeseman, J. R.; Montgomery, J. A., Jr.; Vreven, T.; Kudin, K. N.; Burant, J. C.; Millam, J. M.; Iyengar, S. S.; Tomasi, J.; Barone, V.; Mennucci, B.; Cossi, M.; Scalmani, G.; Rega, N.; Petersson, G. A.; Nakatsuji, H.; Hada, M.; Ehara, M.; Toyota, K.; Fukuda, R.; Hasegawa, J.; Ishida, M.; Nakajima, T.; Honda, Y.; Kitao, O.; Nakai, H.; Klene, M.; Li, X.; Knox, J. E.; Hratchian, H. P.; Cross, J. B.; Bakken, V.; Adamo, C.; Jaramillo, J.; Gomperts, R.; Stratmann, R. E.; Yazyev, O.; Austin, A. J.; Cammi, R.; Pomelli, C.; Ochterski, J. W.; Ayala, P. Y.; Morokuma, K.; Voth, G. A.; Salvador, P.; Dannenberg, J. J.; Zakrzewski, V. G.; Dapprich, S.; Daniels, A. D.; Strain, M. C.; Farkas, O.; Malick, D. K.; Rabuck, A. D.; Raghavachari, K.; Foresman, J. B.; Ortiz, J. V.; Cui, Q.; Baboul, A. G.; Clifford, S.; Cioslowski, J.; Stefanov, B. B.; Liu, G.; Liashenko, A.; Piskorz, P.; Komaromi, I.; Martin, R. L.; Fox, D. J.; Keith, T.; Al-Laham, M. A.; Peng, C. Y.; Nanayakkara, A.; Challacombe, M.; Gill, P. M. W.; Johnson, B.; Chen, W.; Wong, M. W.; Gonzalez, C.; Pople, J. A. *Gaussian 03*, revision D.02; Gaussian, Inc.: Wallingford, CT, 2004.
(19) Nagy, J.; Weaver, D. F., Jr. *Mol. Phys.* **1995**, *85*, 1179–1182.
(20) Meijer, E. J.; Sprik, M. *J. Chem. Phys.* **1996**, *105*, 8684–8689.
(21) Andersson, Y.; Langreth, D. C.; Lundqvist, B. I. *Phys. Rev. Lett.* **1996**, *76*, 102–105.
(22) Kohn, W.; Meir, Y.; Makarov, D. E. *Phys. Rev. Lett.* **1998**, *80*, 4153–4156.
(23) Rowley, R. L.; Pakkanen, T. *J. Chem. Phys.* **1999**, *100*, 3368–3377.
(24) Scott, A. P.; Radom, L. *J. Phys. Chem.* **1996**, *100*, 16502–16513.
(25) Bondi, A. *J. Phys. Chem.* **1964**, *68*, 441–451.
(26) Meng, Z.; Dölle, A.; Carper, W. R. *J. Mol. Struct. (THEOCHEM)* **2002**, *585*, 119–128.
(27) Møller, C.; Plesset, M. S. *Phys. Rev.* **1934**, *46*, 618–622.
(28) Seddon, K. R. Preface. *Ionic Liquids in Synthesis*, 2nd ed.; Wasserscheid, P., Welton, T., Eds.; John Wiley: New York, 2008; Vols. *1 & 2*.

JP809215Z